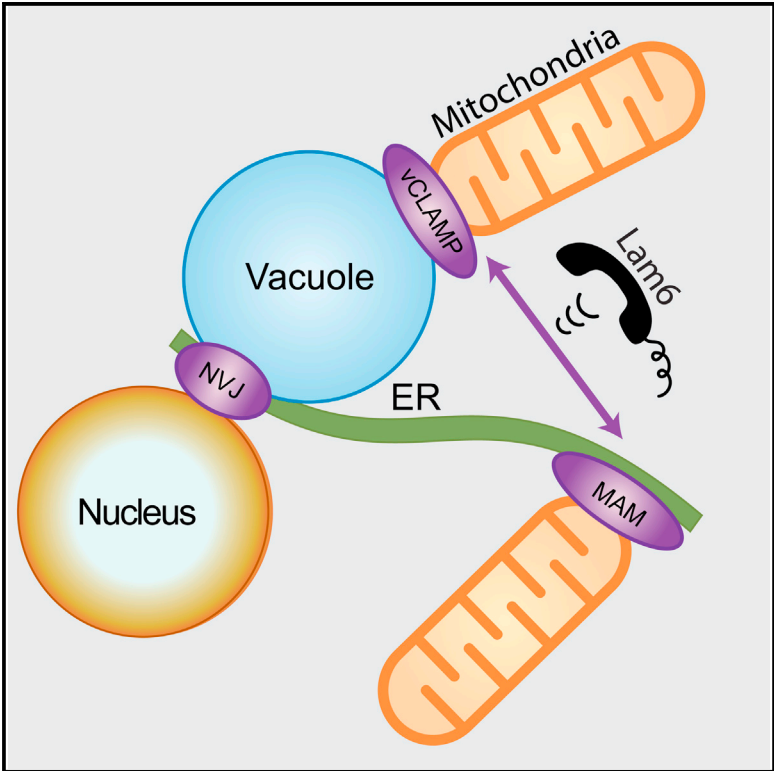


Lam6 Regulates the Extent of Contacts between Organelles

Graphical Abstract



Authors

Yael Elbaz-Alon, Michal Eisenberg-Bord, Vera Shinder, ..., Nils Wiedemann, Tamar Geiger, Maya Schuldiner

Correspondence

maya.schuldiner@weizmann.ac.il

In Brief

Elbaz-Alon et al. find that yeast Lam6, which is part of a conserved protein family, is found in three types of organellar contact sites, ERMES, vCLAMP, and NVJ. Overexpression of Lam6 is sufficient to expand these contact sites and its expression is necessary for cross-regulation of contact site size.

Highlights

- Lam6 is localized to three major cellular contacts: ERMES, vCLAMP, and NVJ
- Lam6 is a GRAM domain protein conserved from yeast to humans
- Overexpression of Lam6 results in the expansion of all three contact sites
- Lam6 is essential for the cross-talk between ERMES and vCLAMP



Lam6 Regulates the Extent of Contacts between Organelles

Yael Elbaz-Alon,^{1,7} Michal Eisenberg-Bord,^{1,7} Vera Shinder,² Sebastian Berthold Stiller,^{3,4} Eyal Shimoni,² Nils Wiedemann,^{3,5} Tamar Geiger,⁶ and Maya Schuldiner^{1,*}

¹Department of Molecular Genetics, Weizmann Institute of Science, Rehovot 7610001, Israel

²Department of Chemical Research Support, Weizmann Institute of Science, Rehovot 7610001, Israel

³Institut für Biochemie und Molekularbiologie, Zentrum für Biochemie und Molekulare Zellforschung (ZBMZ), Universität Freiburg, Freiburg 79104, Germany

⁴Fakultät für Biologie, Universität Freiburg, Freiburg 79104, Germany

⁵BIOS Centre for Biological Signalling Studies, Universität Freiburg, Freiburg 79104, Germany

⁶Department of Human Molecular Genetics and Biochemistry, Tel-Aviv University, Tel Aviv 6997801, Israel

⁷Co-first author

*Correspondence: maya.schuldiner@weizmann.ac.il

<http://dx.doi.org/10.1016/j.celrep.2015.06.022>

This is an open access article under the CC BY-NC-ND license (<http://creativecommons.org/licenses/by-nc-nd/4.0/>).

SUMMARY

Communication between organelles is crucial for eukaryotic cells to function as one coherent unit. An important means of communication is through membrane contact sites, where two organelles come into close proximity allowing the transport of lipids and small solutes between them. Contact sites are dynamic in size and can change in response to environmental or cellular stimuli; however, how this is regulated has been unclear. Here, we show that *Saccharomyces cerevisiae* Lam6 resides in several central contact sites: ERMES (ER/mitochondria encounter structure), vCLAMP (vacuole and mitochondria patch), and NVJ (nuclear vacuolar junction). We show that Lam6 is sufficient for expansion of contact sites under physiological conditions and necessary for coordination of contact site size. Given that Lam6 is part of a large protein family and is conserved in vertebrates, our work opens avenues for investigating the underlying principles of organelle communication.

INTRODUCTION

For eukaryotic cells to function as a coherent unit, organelles must coordinate their function. An important means of communication between organelles is through membrane contact sites, distinct areas where two organelles come into close proximity, allowing the transport of lipids and small solutes (Elbaz and Schuldiner, 2011; Lahiri et al., 2015).

Over the past years, some of the protein tethers that mediate contact sites have been discovered. In the budding yeast, *Saccharomyces cerevisiae*, the first tether to be identified was one that holds together the membranes of the nuclear outer membrane, the ER and the vacuole (the equivalent of the vertebrate lysosome), the NVJ (nuclear vacuolar junction). The pro-

teins creating this tether are Nvj1 on the outer nuclear membrane and Vac8 on the vacuolar membrane (Pan et al., 2000). The next tethering complex to be described forms the contact site between mitochondria and the ER and was named ERMES (ER/mitochondria encounter structure). The ERMES core is composed of three mitochondrial subunits (Mdm34, Mdm12, and Mdm10) and one ER protein (Mmm1) (Kornmann et al., 2009). A third central contact site, the vCLAMP (vacuole and mitochondria patch), has recently been discovered and forms between mitochondria and vacuoles in a manner dependent on Vps39 (Elbaz-Alon et al., 2014; Hönscher et al., 2014).

Contact sites dynamically change in response to environmental and genetic cues (Elbaz and Schuldiner, 2011). For example, the NVJ grows upon entry to stationary growth phase (Pan et al., 2000) and the vCLAMP shrinks during respiratory growth (Hönscher et al., 2014). Moreover, contact sites can be co-regulated: we have shown previously that in the absence of the ERMES complex the vCLAMP expands, and vice versa, thus enabling the cells to maintain homeostasis of the extent of communication through contact sites (Elbaz-Alon et al., 2014). These observations prompt several critical questions. What are the factors that sense cellular cues and translate them into changes in contact site size or composition? How do these regulating factors mediate the remodeling of contact sites? How does remodeling of one contact site affect other contact sites?

In this study, we approached these questions by searching for physically interacting regulators of the ERMES complex. Using mass spectrometry, we discovered that Lam6 (Gatta et al., 2015; Murley et al., 2015) interacts with the ERMES complex, but is not part of the tethering machinery. We show that Lam6 is localized not only to ERMES contact sites but also to the NVJ and vCLAMP. We demonstrate that Lam6 is sufficient to cause the expansion of all three contact sites when highly enriched in them. Moreover, we show that Lam6 is necessary for cross-regulation of contact site size. Importantly, Lam6 is part of a large protein family conserved in evolution from yeast to mammals; thus, our findings open the way for a deeper understanding of one of the fundamental organizational principles in all eukaryotic cells.

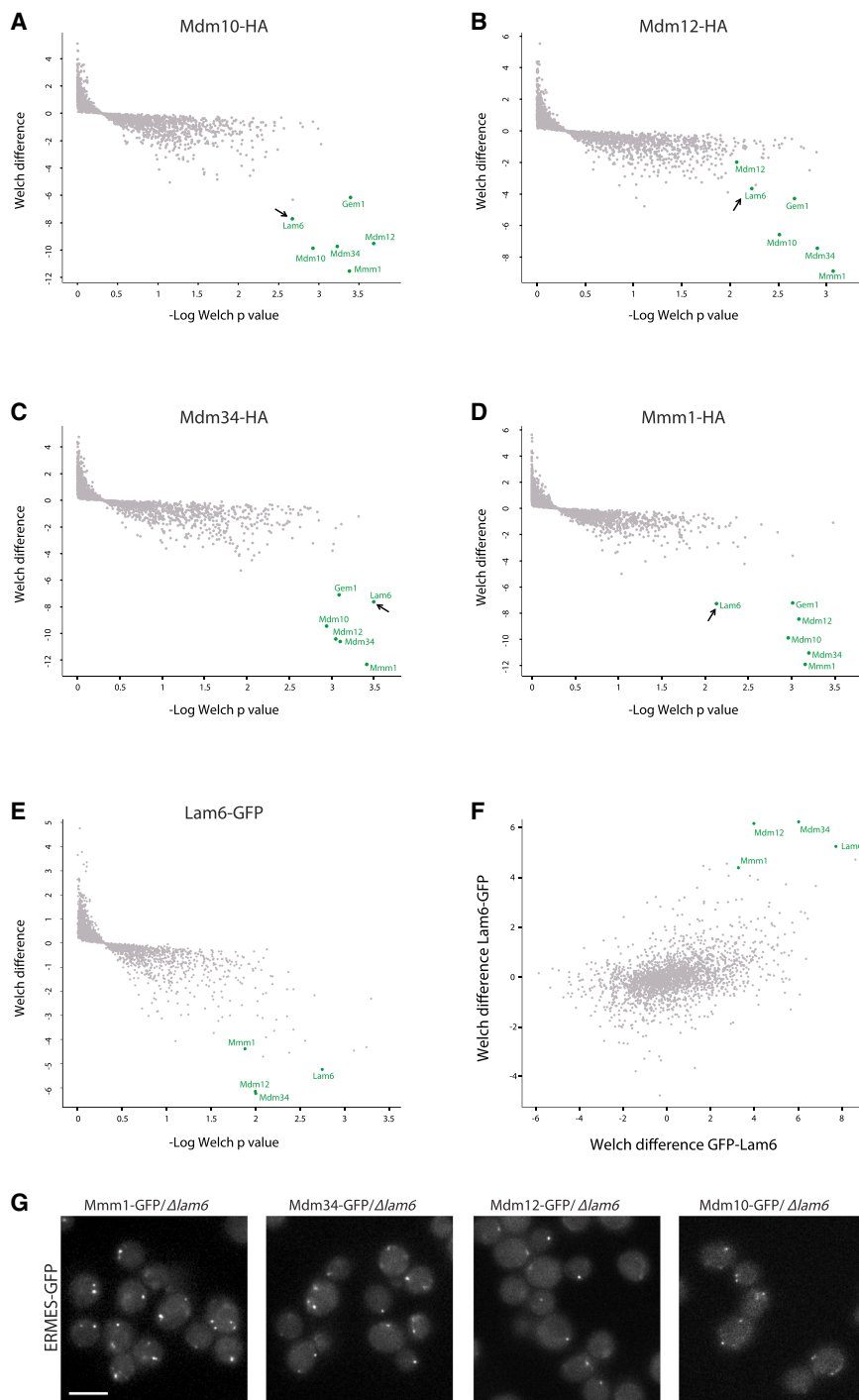


Figure 1. Lam6 Is an Uncharacterized Binding Partner of the ERMES Complex

(A–D) Pull-down of HA-tagged ERMES components (Mdm10, A; Mdm12, B; Mdm34, C; and Mmm1, D) uncovered that all ERMES components interact with the same uncharacterized protein, Lam6. Lam6 and members of the ERMES complex are marked in green.

(E–F) Reciprocal pull-down demonstrated that endogenously expressed C-terminally tagged Lam6 (E) and overexpressed N-terminally tagged Lam6 (F) have the same strong binding partners that include the ERMES complex members (G). GFP-tagged ERMES complex proteins retain their characteristic punctate structure in $\Delta lam6$, suggesting that Lam6 is not an essential complex member. Scale bar represents 5 μ m.

Mdm34, Mdm10, and Mdm12). As expected, each ERMES subunit showed strong interaction with the three other subunits, as well as with Gem1, a previously characterized interactor (Kornmann et al., 2011; Stroud et al., 2011). In addition to the known binding partners, all ERMES components interacted with Lam6 (Figures 1A–1D); the complete list of interactors is given in Table S1).

To verify the interaction of the ERMES complex members with Lam6, we performed pull-down experiments on a genomic version of C-terminally GFP-tagged Lam6 under its own promoter, as well as an N-terminally tagged strain in which Lam6 is overexpressed. Mass spectrometry analysis confirmed that, regardless of the position of the GFP or the levels of expression, Lam6 bound strongly to three of the ERMES complex subunits (Mdm34, Mdm12, and Mmm1; Figures 1E and 1F) and, to a lesser extent, to Mdm10 and Gem1 (a full list of significant interactors is given in Table S2).

We wondered if Lam6, as a strong ERMES binding partner, is an essential member of the complex. The absence of any of the core ERMES subunits results in disassociation of the complex and redistribution of the other subunits from a punctate pattern to a uniform

localization along the entire organelle of residence (Kornmann et al., 2009). However, in strains lacking Lam6 ($\Delta lam6$), all four GFP-tagged ERMES subunits displayed normal punctate structures (Figure 1G) and normal mitochondrial protein levels (Figure S1A).

Moreover, deletion of any of the ERMES subunits did not alter the punctate pattern of Lam6-GFP, suggesting that the ERMES complex is not important for its recruitment (Figure S1B). In

RESULTS

Lam6 Is an Uncharacterized Binding Partner of the ERMES Complex

To try and uncover regulators of contact site dynamics, we set out to identify novel binding partners for ERMES proteins. To this end, we performed a pull-down followed by mass spectrometry analysis of the four subunits of the complex (Mmm1,

addition, unlike ERMES mutants, which are characterized by having abnormal mitochondria shape, impaired growth rate, and an inability to grow on a non-fermentable carbon source (Kornmann et al., 2009), loss of *LAM6* did not affect growth on either a fermentable or non-fermentable carbon source (Figure S1C), mitochondrial morphology (Figure S1D), or the levels of a variety of mitochondrial proteins (Figure S1A). Interestingly, overexpressing Lam6 had no effect on growth or mitochondrial morphology, even on the background of Δ *mdm34* (Figures S1C and S1D). Altogether, this suggests that Lam6 is not required for the formation of the ERMES complex, hinting at a regulatory role for this interaction.

Lam6 Is Localized to Several Cellular Contact Sites

Given that Lam6 physically associated with the ERMES complex and Lam6-GFP strains demonstrated punctate fluorescence, we assayed whether Lam6 localized to ERMES-mediated contact sites. Indeed, the majority of Lam6-GFP signal co-localized with ERMES foci (marked by Cherry-Mdm34) (Figure 2A, yellow arrows). However, we noticed that some of the Lam6-GFP signal was in non-ERMES structures (Figure 2A, red arrow). This observation, coupled with the fact that one of the physical interactors of Lam6 was the NVJ contact site protein Vac8 (Table S2), implied that Lam6 might reside in additional contact sites. We, therefore, co-localized Lam6 C-terminally tagged with Cherry (Lam6-Cherry) with two additional contact site markers: Nvj1-GFP (marking the NVJ) and GFP-Vps39 (marking the vCLAMP). Although most Lam6 puncta co-localized with ERMES markers, we also could detect co-localization with the other contact site markers, demonstrating that Lam6 has a wider contact site distribution (Figure 2A).

To confirm this co-localization, we repeated it using a strain in which Lam6 is overexpressed. Despite efforts to overexpress Lam6-GFP by changing the endogenous promoter to a strong constitutive promoter, we could not get an increase in protein levels (Figure S2). We, therefore, turned to the N-terminally tagged overexpressed version shown to have a similar pattern of physical interactions as the endogenously expressed one (Figure 1F). Indeed, overexpressed GFP-Lam6 or Cherry-Lam6 displayed a dramatic increase in the amount of protein in each of the three contact sites (Figures 2B and S2). Although Lam6 levels were higher now, Lam6 was still localized in a specific manner to the three membrane contact sites.

Overexpression of Lam6 Affects the Extent of Contact Sites

When visualizing the overexpressed GFP-Lam6 or Cherry-Lam6, we noticed a dramatic accumulation of Lam6 in the three major cellular contact sites, ERMES, NVJ, and vCLAMP. We wondered whether the strong signals that we were obtaining were merely a result of the abundance of Lam6 or whether the contact sites themselves were changing. We, therefore, visualized all three contact sites, ERMES (Mdm34-GFP), NVJ (Nvj1-GFP), and vCLAMP (GFP-Vps39), in the absence (Δ *lam6*), overexpression (*OE-LAM6*), or overexpression and N-terminally tagging (*OE-Cherry-LAM6*) of the protein.

As was the case for the ERMES complex, the absence of Lam6 did not affect the integrity of the NVJ or vCLAMP, suggesting that

Lam6 is not essential for the formation of any of the contact sites examined (Figure S3A).

Although replacing the endogenous promoter with a strong promoter alone did not result in a change in contact site appearance (Figure S3B), we could observe a dramatic effect when N'-tagged Lam6 was overexpressed and accumulated in contact sites. Under these conditions, all the three contact sites assayed expanded between 1.5- to 6-fold in size (Figure 3A), suggesting that the increased levels of Lam6 in these contacts were enough to cause their expansion.

To further study the expanded contacts, we used electron microscopy (EM). Consistent with fluorescence microscopy images, replacing the promoter with a stronger one alone was not enough to cause expansion of contact sites (Figure S3C). However, we could indeed observe a dramatic expansion when the N'-tagged Lam6 strain was overexpressed. Specifically, when we looked at strains in which Lam6 was endogenously expressed and C-terminally tagged with GFP (using immune-labeling against GFP), the various contact sites within the cell were rare and small. Furthermore, under these conditions, we could only find a small number of Lam6 gold particles per cell (matching the low and localized fluorescence signal of the same strain; Figure 3B). Distribution analysis of gold particles showed that, in the majority of cases (80%), endogenously expressed Lam6 was localized to mitochondria (Figure S3D).

In comparison, in strains in which GFP-Lam6 was overexpressed, we could detect a larger number of gold particles that were distributed among all three contact sites. Importantly, this resulted in a dramatic effect on the morphology and extent of all three contact sites (Figure 3B).

Instances in which vacuoles and mitochondria were found in close proximity were markedly higher in Lam6-overexpressing cells. Interestingly, the vCLAMPs (validated by immuno-labeling Vps39; Figure S3E) were invaded by tubules of ER, potentially due to the fact that a large fraction of the mitochondrial surface was now covered in ER tubules (see below).

The NVJ contact site was not only expanded upon overexpression of GFP-Lam6, but now also displayed a phenomenon never seen in control cells. Patches of the nucleus that expressed GFP-Lam6 were engulfed by the vacuole (Figure 3B), in a process resembling piecemeal microautophagy of the nucleus (PMN) (Roberts et al., 2003).

However, the most dramatic phenotype resulting from GFP-Lam6 overexpression was seen in the ER/mitochondria contact site. Higher amounts of Lam6 in the contact site resulted in its elongation, in comparison to the distinct contact seen under endogenous Lam6 levels. ER tubules now surrounded mitochondria. Quantifying this effect, we found that the percentage of mitochondria found in close proximity to the ER was much higher in the strain overexpressing GFP-Lam6 than in the wild-type (WT) strain (88.5% versus 25%, respectively; Figure S3F). Moreover, in the overexpression strain, the ER covered more of the mitochondria's circumference than in the WT (average coverage of 61% and 17%, respectively; Figure S3G). These additional membranes were not due to autophagy, as GFP-Atg8 Foci did not increase (Figure S3H). Altogether, the EM analysis indicates that high levels of Lam6 in specific contact sites are sufficient to modulate contact site extent.

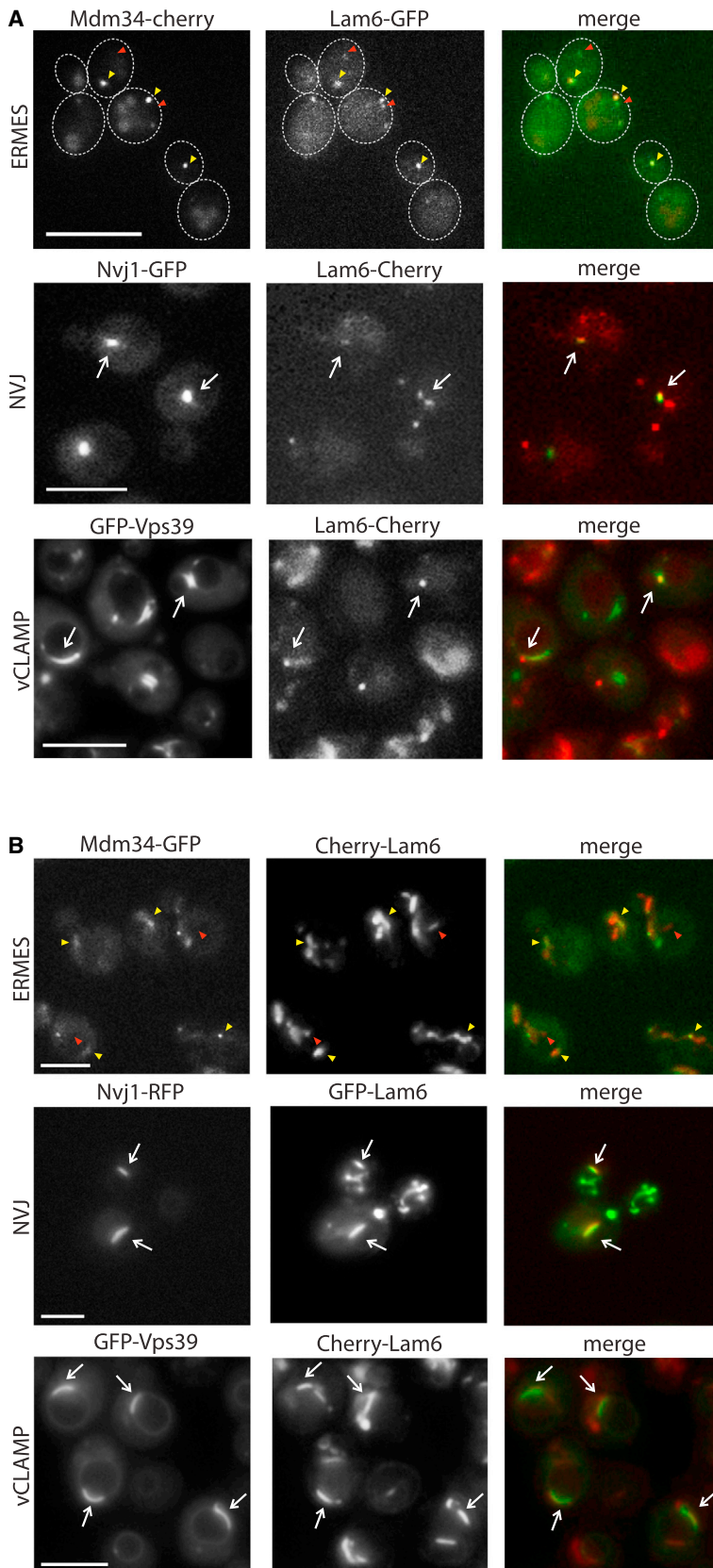


Figure 2. Lam6 Is Localized to Several Cellular Contact Sites

(A) Fluorescence microscopy demonstrates that Lam6-GFP co-localizes with ERMES (Mdm34-Cherry) (yellow arrows) and also localizes to non-ERMES locations in the cell (red arrows). These additional locations co-localized with the NVJ (Nvj1-GFP) as well as with the vCLAMP (GFP-Vps39). Scale bar represents 5 μ m.

(B) Overexpression and tagging of Lam6 confirmed that it co-localizes with ERMES (Mdm34-GFP) (yellow arrows) as well as to additional contact sites (red arrows), NVJ (marked by Nvj1) and vCLAMP (marked by Vps39). Scale bar represents 5 μ m.

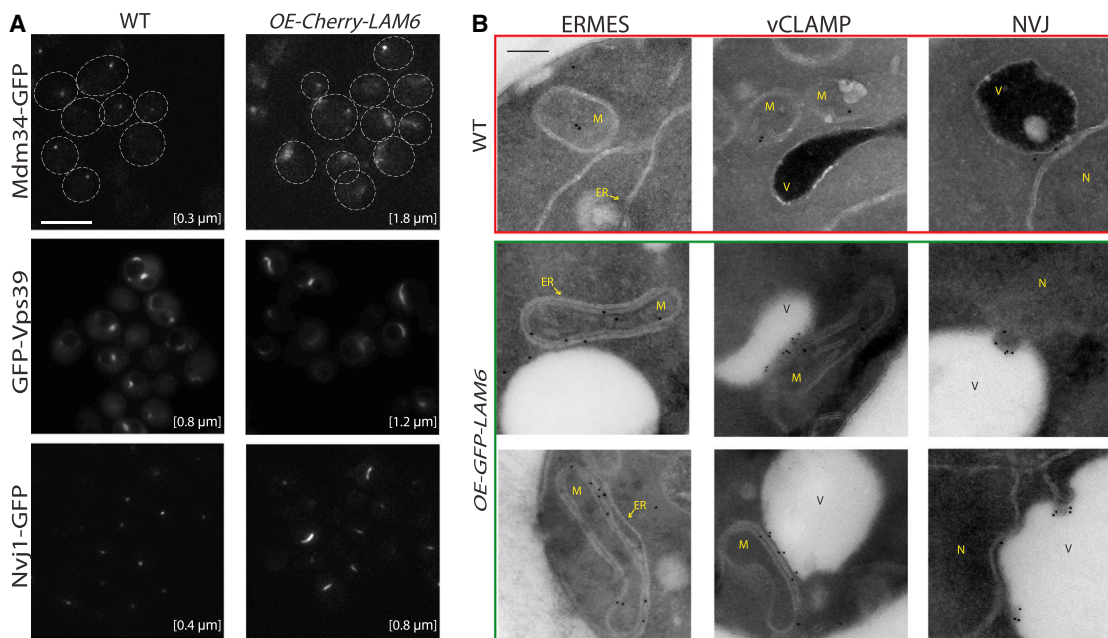


Figure 3. Overexpression and Tagging of Lam6 Affects the Extent of Contact Sites

(A) Fluorescence microscopy demonstrates that the overexpression of Cherry-Lam6 (*OE-Cherry-LAM6*) results in an expansion of the following three contact sites: ERMES (Mdm34-GFP), NVJ (Nvj1-GFP), and vCLAMP (GFP-Vps39). This suggests that an increase in Lam6 levels in the contact site is sufficient for its expansion. The numbers represent the average contact site size (120 cells per sample). Scale bar represents 5 μm.

(B) Immuno-EM verified that GFP-Lam6 overexpression indeed causes an expansion of contact site size. While vCLAMP was hardly visible in WT cells, it could be detected easily in the OE strain (albeit often had ER tubules invading it). The NVJ underwent expansion as well as evoked PMN in OE strains, and the ER-mitochondria contact became large and elongated instead of small and distinct. N, nucleus; M, mitochondria; V, vacuole. Scale bar represents 200 nm (see also Figure S3I).

Lam6 Is Important for Cross-Talk between Contact Sites

Given that higher levels of Lam6 in contact sites were sufficient to affect the degree of interaction between organelles, we wondered if it takes part in the expansion of contact sites under physiological conditions, a process whose mechanism remains unknown. We have shown previously that, in the absence of the vCLAMP, the extent of ERMES junctions per cell increases, and vice versa (Elbaz-Alon et al., 2014). We thus set out to investigate whether Lam6 is necessary for this known physiological expansion of a contact site. Using fluorescence microscopy, we assayed the requirement for Lam6 in lengthening ERMES (marked by Mdm34-GFP) in the absence of the vCLAMP ($\Delta vps39$). In the absence of vCLAMP, there was a marked increase in the number of visible Mdm34-GFP- or Mmm1-GFP-marked contact sites per cell when compared to the WT background. Remarkably, in the absence of Lam6, there was no increase in the number of visible contacts (verified to be on mitochondria; Figure S4A) upon loss of vCLAMP (Figure 4A and quantification in Figures 4B and S4B and quantification in Figure S4C, respectively).

To see if Lam6 also was taking part in the expansion of vCLAMP when the ERMES complex had been compromised, we performed the reciprocal experiment. Visualizing vCLAMP by GFP-Vps39, we easily could see that reducing ERMES contacts (by growing *GALP-MDM34* strains on glucose) caused the expansion of GFP-Vps39 foci, but this phenomenon was dependent on the presence of Lam6 (Figure 4C). Hence, Lam6 is both necessary and sufficient for contact site expansion,

and it is important for the coordination between these two contact sites. Such cross-talk should enable the cell to compensate for loss of one contact by the expansion of the other, allowing dynamic regulation and maintenance of intracellular connectivity.

The co-regulation of ERMES and vCLAMP is essential for cell viability. Indeed, tetrad analysis confirmed that double mutants for $\Delta lam6$ and mutants in any of the ERMES subunits had a synthetic sick phenotype (Figure S4D). Interestingly, mutants for Lam6 and Vps39 were not synthetic sick. We hypothesize that this is because, in the absence of vCLAMP, ERMES contacts, always present in two to three sites in logarithmically growing cells, are enough to sustain growth without expanding. On the other hand, vCLAMPs, rarely seen in cells with normal ERMES connections or at regular expression levels of Vps39, are not able to sustain growth if unable to expand dramatically during loss of ERMES.

Together our data suggest a central role for Lam6 in regulating the cross-talk between the various cellular contact sites, enabling the cell to maintain an optimal flow of information and solutes by regulating the extent of contacts between organelles.

DISCUSSION

Membrane contact sites, which serve as essential relaying points of both building blocks and signals, are known to be dynamic and affected by various cellular cues. In this study, we uncovered an uncharacterized contact site protein, Lam6, which is conserved

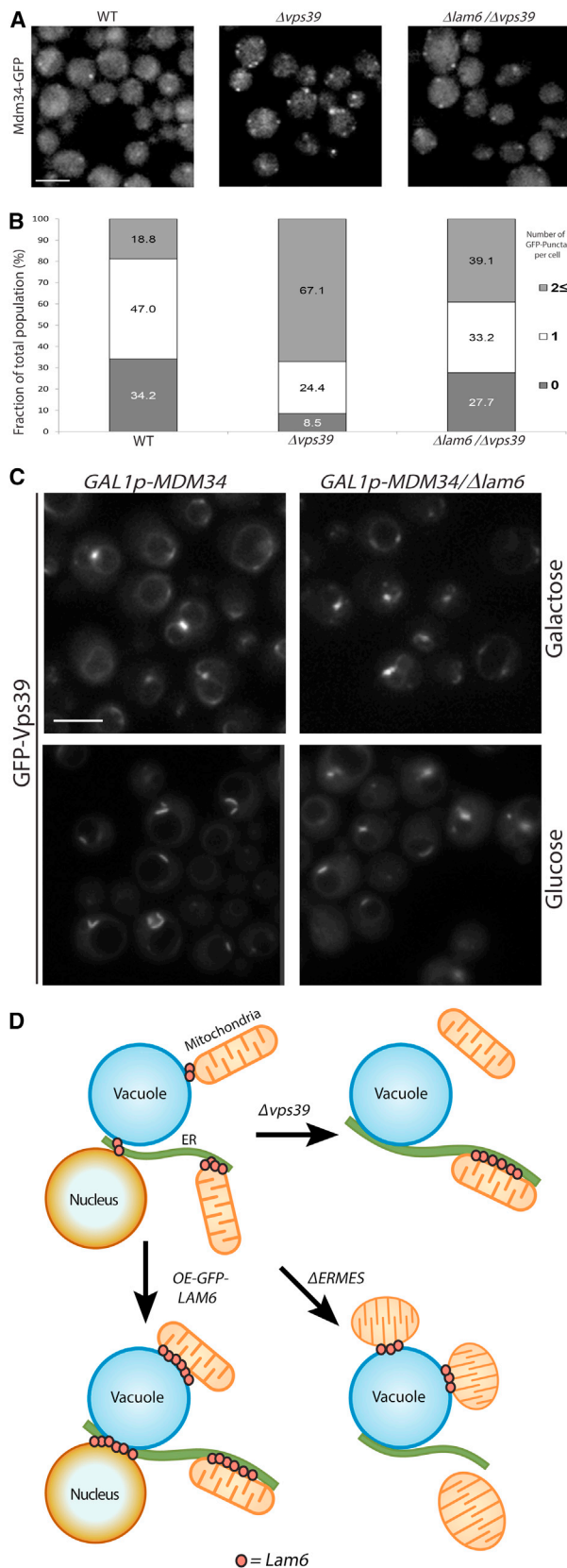


Figure 4. Lam6 Is Important for Cross-Talk between Contact Sites

(A) Fluorescent microscopy shows that the ERMES contact (as measured by the number of Mdm34-GFP puncta per cell) expanded in the $\Delta vps39$ background relative to WT. However, the expansion did not occur on the background of $\Delta vps39 \Delta lam6$, demonstrating that Lam6 is necessary for ERMES expansion under these conditions. Scale bar represents 5 μ m.

(B) Quantitation of (A). Bars represent the percentage of cells containing the specific number of puncta/cell out of total cells counted for the strain (for WT, n = 234 cells; for $\Delta vps39$, n = 246; for $\Delta vps39 \Delta lam6$, n = 271).

(C) Fluorescent microscopy demonstrates that downregulating ERMES contacts (by growing *GAL1p-MDM34* strains in glucose) indeed caused expansion of vCLAMP (GFP-Vps39). However, this expansion was diminished in a $\Delta lam6$ background. Scale bar represents 5 μ m (see also Figure S4).

(D) A model summarizing our hypothesis on the way that Lam6 functions to regulate contact site communication. In normal cells, where all contact sites are intact, Lam6 is found mostly in ERMES contact sites, and to a lesser extent in vCLAMP and NVJ. However, in case a contact site is lost, the Lam6 proteins that were localized to this contact become free to associate with the other contact sites, thus signaling that they must expand. Raising Lam6 levels in any other way in a contact site therefore would cause an expansion of this contact site.

from yeast to mammals. Lam6 is localized to three major cellular contacts, ERMES, vCLAMP, and NVJ (Gatta et al., 2015; Murley et al., 2015). Our results demonstrate, however, that Lam6 is not required for contact site formation, posing it as a regulatory protein. Importantly, higher levels of Lam6 in contact sites resulted in a dramatic expansion of all three contact sites, indicating that the levels of Lam6 in contact sites are the limiting factor for the extent of each contact. We also show that Lam6 is essential for the co-regulation of ERMES and vCLAMP, highlighting it as a central regulator in determining the levels of communication between organelles (Figure 4). In the future, it will be interesting to study the role of Lam6 in the cross-talk and co-regulation of these two contact sites with the NVJ.

How might Lam6 function to regulate contact site extent? As overall Lam6 protein levels were not changed upon the deletion of ERMES (data not shown), we believe that it is the distribution of Lam6 between contact sites and its local concentration in them that affect their extent. One simple model would be that Lam6 has differential affinities for the three contact sites. In normal cells, where all contact sites are intact, Lam6 is found mostly in ERMES contact sites, and to a lesser extent in vCLAMP and NVJ. However, in case a contact site is lost, the Lam6 proteins that were localized to this contact become free to associate with the other contact sites, thus signaling that they must expand. Raising Lam6 levels in any other way in a contact site therefore would cause an expansion of this contact site (Figure 4D), fitting with our observations. Given that the overexpression of the C'-tagged form of Lam6 did not result in higher levels of the protein, whereas overexpression of the N'-tagged form did, it is appealing to speculate that the turnover of tagged Lam6 is slower when its N terminus is blocked by a tag. Hence, post-translational modification of the N' of Lam6 or binding of this domain by other proteins may be the mechanism by which Lam6 levels are regulated to expand contact sites in vivo. In the future, it would be exciting to determine what is the molecular mechanism by which Lam6 is recruited to specific contact sites and expands them, as well as what are the regulatory cascades linking Lam6 to cellular condition and energy demands.

An important first clue for the recruitment of Lam6 comes from our finding that deletion of one of the strong interactors of Lam6 (Table S2), the mitochondrial outer membrane protein Tom71 (a subunit of the translocase of the outer membrane [TOM] complex) and its close homolog Tom70 completely rerouted Lam6 from the ER-mitochondria junction (marked by Mdm34) to the NVJ (marked by Nvj1; Figure S4E). Therefore, Tom70/71 are essential for recruitment of Lam6 to its location on mitochondria, and mitochondrial import may serve as a regulatory switch for contact site formation.

To date, few regulatory molecules overseeing the dynamics of contact sites have been identified, and thus there is still much to uncover in this field. The number of known contact sites within the cell continues to grow and new contact sites that are condition specific are still being discovered. Therefore, it is likely to assume that more contact site regulators exist and have yet to be found. Understanding the mechanisms by which these regulators sense general cellular cues and translate them into changes in contact site size, and how these proteins regulate expansion or contraction of contact sites, is an important step in the understanding of the communication between organelles. Moreover, identifying novel multi-site regulators also could be used to identify new contact sites.

Lam6 is a member of a family of proteins (Ysp1, Ysp2, Sip3, Lam4, Lam5, and Lam6) (Gatta et al., 2015) that share a GRAM lipid-binding domain (Doerks et al., 2000). It will be interesting to determine the role of this domain in the function of Lam6. In addition, it will be interesting to check if the other members of the family also have a regulatory function in the various contact sites. Unlike the ERMES complex, Lam6 is conserved to mammalian cells, and has two mammalian homologs: GRAMD1a and GRAMD1c, which are also GRAM domain-containing proteins. This conservation may open the way to uncovering additional mammalian contact site tethers using yeast-gleaned knowledge, thereby providing a stepping stone to new understandings of intracellular communication in eukaryotic cells in general.

EXPERIMENTAL PROCEDURES

Strains and Plasmids

Strains created in this study are listed in Table S3. All yeast strains in this study were based on the BY4741 laboratory strains (Brachmann et al., 1998). Genetic manipulations were performed using the lithium acetate, polyethylene glycol (PEG), single-stranded DNA (ssDNA) method for transforming yeast strains (Gietz and Woods, 2006), using integration plasmids previously described in Longtine et al. (1998). For staining of mitochondria, we used an MTS-RFP plasmid (kindly provided by Jodi Nunnari). For GFP-Atg8 quantification, we used a GFP-Atg8 plasmid (kindly provided by Zvulun Elazar).

Manual Fluorescence Microscopy

Imaging was performed using an Olympus IX71 microscope controlled by the DeltaVision SoftWoRx 3.5.1 software with $\times 60$ or $\times 100$ oil lens. Images were captured by a Photometrics Coolsnap HQ camera with excitation at 490/20 nm and emission at 528/38 nm (GFP) and excitation at 555/28 nm and emission at 617/73 nm (mCherry/RFP). Images were transferred to Adobe Photoshop CS3 for slight contrast and brightness adjustments.

EM

For immuno-EM, cells were fixed in 4% paraformaldehyde with 0.1% glutaraldehyde in 0.1 M cacodylate buffer (pH = 7.4). Contrasting and embedding

were performed as described previously (Tokuyasu, 1986). For more details, see the Supplemental Experimental Procedures.

Isolation of Microsomal Fractions

Pull-downs of individual ERMES components (Mmm1-3HA, Mdm34-3HA, Mdm12-3HA, and Mdm10-3HA) for liquid chromatography-tandem mass spectrometry (LC-MS/MS) were performed from microsomal fractions. Sucrose-density-gradient purification of microsomes was performed essentially as described by Wuestehube and Schekman (1992). For more details, see the Supplemental Experimental Procedures.

Isolation of Mitochondria-Enriched Fractions

Pull-down of Lam6-GFP and GFP-Lam6 for LC-MS/MS analysis was performed from mitochondria-enriched preparations. Isolation of mitochondria-enriched fractions was performed essentially as described previously (Daum et al., 1982). For more details, see the Supplemental Experimental Procedures.

Interaction Proteomics

LC-MS/MS analysis was performed on the EASY-nLC1000 UHPLC (Thermo Scientific) coupled to the Q-Exactive mass spectrometer (Thermo Scientific). Significant interactors were extracted based on the statistical difference between the label-free quantification (LFQ) intensities of the proteins in the pull-down of specific proteins and the control strains without hemagglutinin (HA)-tag expression. One-sided Welch's test was performed with 0.05 permutation-based FDR and $S_0 = 0.5$ (Tusher et al., 2001). For more details, see the Supplemental Experimental Procedures.

SUPPLEMENTAL INFORMATION

Supplemental Information includes Supplemental Experimental Procedures, four figures, and three tables and can be found with this article online at <http://dx.doi.org/10.1016/j.celrep.2015.06.022>.

AUTHOR CONTRIBUTIONS

Y.E.-A. and M.E.-B. performed the majority of the experiments. V.S. and E.S. performed the EM analysis. T.G. performed the mass spectrometric analysis. S.B.S. and N.W. performed the biochemistry on isolated mitochondria in WT and deletion mutants. Y.E.-A., M.E.-B., and M.S. conceived the ideas and wrote the manuscript.

ACKNOWLEDGMENTS

We thank Lihi Gal and Silvia Chuartzman for technical assistance. We are grateful to Oren Elbaz for graphic design. We thank Oren Schuldiner, Cory Dunn, Einat Zalckvar, Naama Aviram, and Tslil Ast for critical reading of the manuscript. We thank Jodi Nunnari and Zvulun Elazar for plasmids. M.S., Y.E.-A., and M.E.-B. were funded by the European Research Council (ERC) Starting Grant 260395. N.W. was supported by the Sonderforschungsbereich 1140 and the Excellence Initiative of the German federal and state governments (EXC 294 BIOS). T.G. was funded by the Israel Cancer Research Fund. The EM studies were conducted at the Irving and Cherna Moskowitz Center for Nano and Bio-Nano Imaging (Weizmann Institute of Science).

Received: February 11, 2015

Revised: May 10, 2015

Accepted: June 8, 2015

Published: June 25, 2015

REFERENCES

Brachmann, C.B., Davies, A., Cost, G.J., Caputo, E., Li, J., Hieter, P., and Boeke, J.D. (1998). Designer deletion strains derived from *Saccharomyces cerevisiae* S288C: a useful set of strains and plasmids for PCR-mediated gene disruption and other applications. *Yeast* 14, 115–132.

- Daum, G., Böhni, P.C., and Schatz, G. (1982). Import of proteins into mitochondria. Cytochrome b2 and cytochrome c peroxidase are located in the intermembrane space of yeast mitochondria. *J. Biol. Chem.* **257**, 13028–13033.
- Doerks, T., Strauss, M., Brendel, M., and Bork, P. (2000). GRAM, a novel domain in glucosyltransferases, myotubularins and other putative membrane-associated proteins. *Trends Biochem. Sci.* **25**, 483–485.
- Elbaz, Y., and Schuldiner, M. (2011). Staying in touch: the molecular era of organelle contact sites. *Trends Biochem. Sci.* **36**, 616–623.
- Elbaz-Alon, Y., Rosenfeld-Gur, E., Shinder, V., Futerman, A.H., Geiger, T., and Schuldiner, M. (2014). A dynamic interface between vacuoles and mitochondria in yeast. *Dev. Cell* **30**, 95–102.
- Gatta, A.T., Wong, L.H., Sere, Y.Y., Calderón-Noreña, D.M., Cockcroft, S., Menon, A.K., and Levine, T.P. (2015). A new family of StART domain proteins at membrane contact sites has a role in ER-PM sterol transport. *eLife* **4**, e07253.
- Gietz, R.D., and Woods, R.A. (2006). Yeast transformation by the LiAc/SS Carrier DNA/PEG method. *Methods Mol. Biol.* **313**, 107–120.
- Hönscher, C., Mari, M., Auffarth, K., Bohnert, M., Griffith, J., Geerts, W., van der Laan, M., Cabrera, M., Reggiori, F., and Ungermann, C. (2014). Cellular metabolism regulates contact sites between vacuoles and mitochondria. *Dev. Cell* **30**, 86–94.
- Kornmann, B., Currie, E., Collins, S.R., Schuldiner, M., Nunnari, J., Weissman, J.S., and Walter, P. (2009). An ER-mitochondria tethering complex revealed by a synthetic biology screen. *Science* **325**, 477–481.
- Kornmann, B., Osman, C., and Walter, P. (2011). The conserved GTPase Gem1 regulates endoplasmic reticulum-mitochondria connections. *Proc. Natl. Acad. Sci. USA* **108**, 14151–14156.
- Lahiri, S., Toulmay, A., and Prinz, W.A. (2015). Membrane contact sites, gateways for lipid homeostasis. *Curr. Opin. Cell Biol.* **33**, 82–87.
- Longtine, M.S., McKenzie, A., 3rd, Demarini, D.J., Shah, N.G., Wach, A., Brachat, A., Philippsen, P., and Pringle, J.R. (1998). Additional modules for versatile and economical PCR-based gene deletion and modification in *Saccharomyces cerevisiae*. *Yeast* **14**, 953–961.
- Murley, A., Sarsam, R.D., Toulmay, A., Yamada, J., Prinz, W.A., and Nunnari, J. (2015). Ltc1 is an ER-localized sterol transporter and a component of ER-mitochondria and ER-vacuole contacts. *J. Cell Biol.* **209**, 539–548.
- Pan, X., Roberts, P., Chen, Y., Kvam, E., Shulga, N., Huang, K., Lemmon, S., and Goldfarb, D.S. (2000). Nucleus-vacuole junctions in *Saccharomyces cerevisiae* are formed through the direct interaction of Vac8p with Nvj1p. *Mol. Biol. Cell* **11**, 2445–2457.
- Roberts, P., Moshitch-Moshkovitz, S., Kvam, E., O'Toole, E., Winey, M., and Goldfarb, D.S. (2003). Piecemeal microautophagy of nucleus in *Saccharomyces cerevisiae*. *Mol. Biol. Cell* **14**, 129–141.
- Stroud, D.A., Oeljeklaus, S., Wiese, S., Bohnert, M., Lewandrowski, U., Sickmann, A., Guiard, B., van der Laan, M., Warscheid, B., and Wiedemann, N. (2011). Composition and topology of the endoplasmic reticulum-mitochondria encounter structure. *J. Mol. Biol.* **413**, 743–750.
- Tokuyasu, K.T. (1986). Application of cryoultramicrotomy to immunocytochemistry. *J. Microsc.* **143**, 139–149.
- Tusher, V.G., Tibshirani, R., and Chu, G. (2001). Significance analysis of microarrays applied to the ionizing radiation response. *Proc. Natl. Acad. Sci. USA* **98**, 5116–5121.
- Wuestehube, L.J., and Schekman, R.W. (1992). Reconstitution of transport from endoplasmic reticulum to Golgi complex using endoplasmic reticulum-enriched membrane fraction from yeast. *Methods Enzymol.* **219**, 124–136.

Cell Reports

Supplemental Information

Lam6 Regulates the Extent of Contacts between Organelles

Yael Elbaz-Alon, Michal Eisenberg-Bord, Vera Shinder, Sebastian Berthold Stiller, Eyal Shimoni, Nils Wiedemann, Tamar Geiger, and Maya Schuldiner

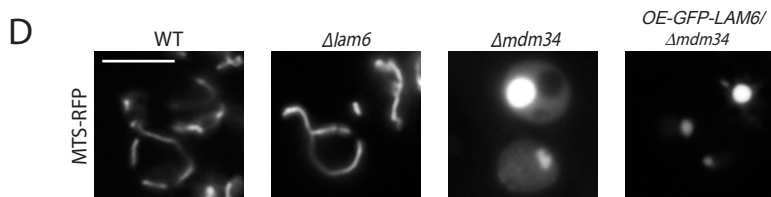
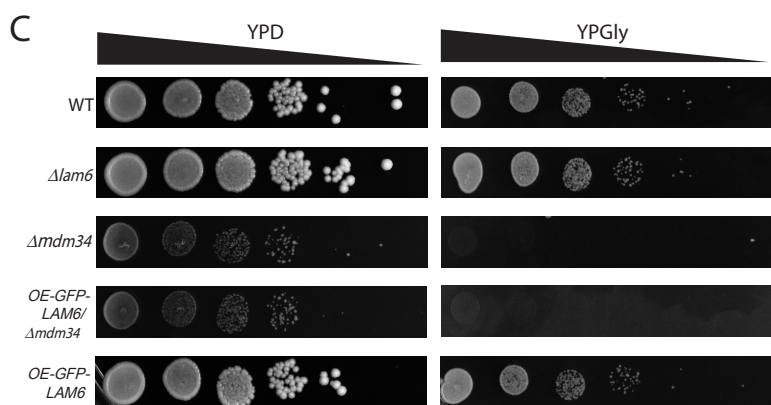
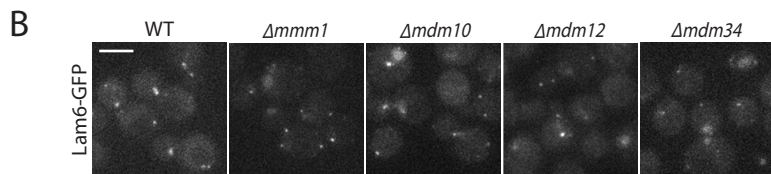
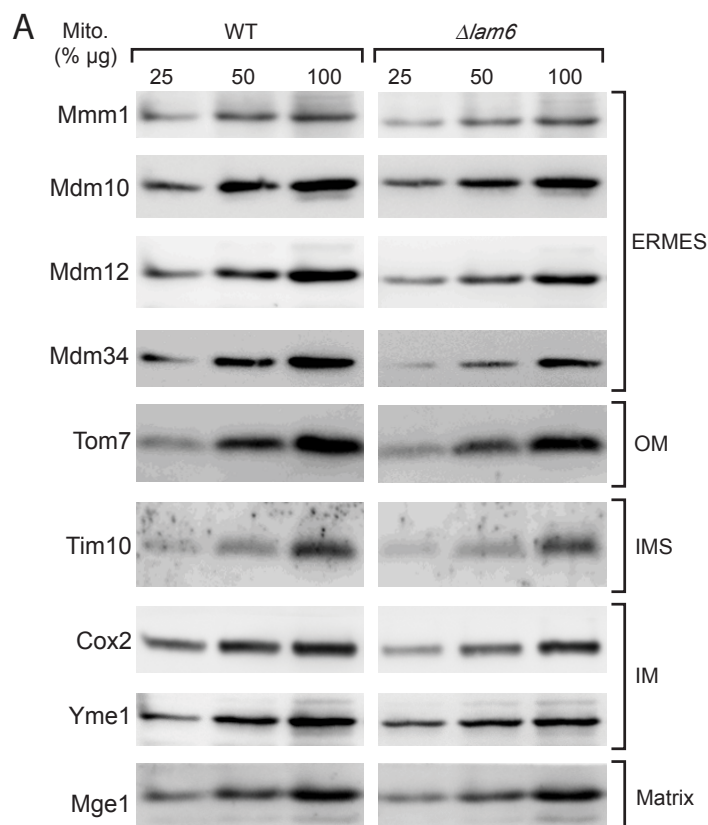


Figure S1: Lam6 is an uncharacterized binding partner of the ERMES complex. Related to figure 1.

(A) ERMES complex proteins remain in similar abundance following loss of Lam6 as do other mitochondrial proteins. Mitochondria were isolated from the yeast strains indicated. Mitochondrial proteins (% μg protein) were analyzed by SDS-PAGE and Western blotting. OM, outer membrane; IMS, intermembrane space; IM, inner membrane. (B) Deletion of any of the ERMES subunits did not result in a change in Lam6-GFP punctate structure, implying that it is not an essential part of the ERMES complex. Bar = 5 μm . (C) Serial dilutions of yeast strains demonstrate that unlike the *ERMES* mutant- Δmdm34 , *LAM6* mutants displayed normal growth on a fermentable (YPD_{extrose}) as well as a non-fermentable carbon source (YPGly_{cerol}). (D) *LAM6* mutants have a normal mitochondrial shape, in contrast to the *ERMES* mutant Δmdm34 . Overexpression of GFP-Lam6 did not affect the growth of a Δmdm34 strain (C) as well as its mitochondria's shape (D). Bar = 5 μm .

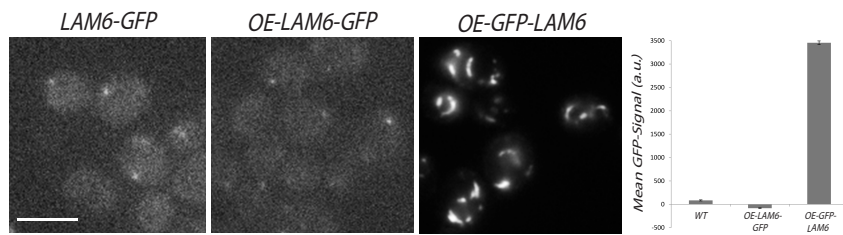


Figure S2: Tagging of Lam6 at its N' stabilizes the protein. Related to figure 2.

Replacing the endogenous promoter of C-terminally-GFP-tagged Lam6 with a constitutive promoter (*OE-LAM6-GFP*) did not affect the punctuate pattern of the protein, nor elevated the fluorescence GFP signal, implying that the protein was not overexpressed. However, replacing the promoter of an N-terminally-GFP-tagged Lam6 with a constitutive promoter (*OE-GFP-LAM6*) resulted in a robust, elevated GFP signal and the protein could be now seen clearly at the different contact sites. Flow cytometry was used in order to evaluate GFP-tagged Lam6 levels, bars are mean GFP-intensity (arbitrary units) normalized to the background signal of an untagged strain, n=3. Bar = 5 μm .

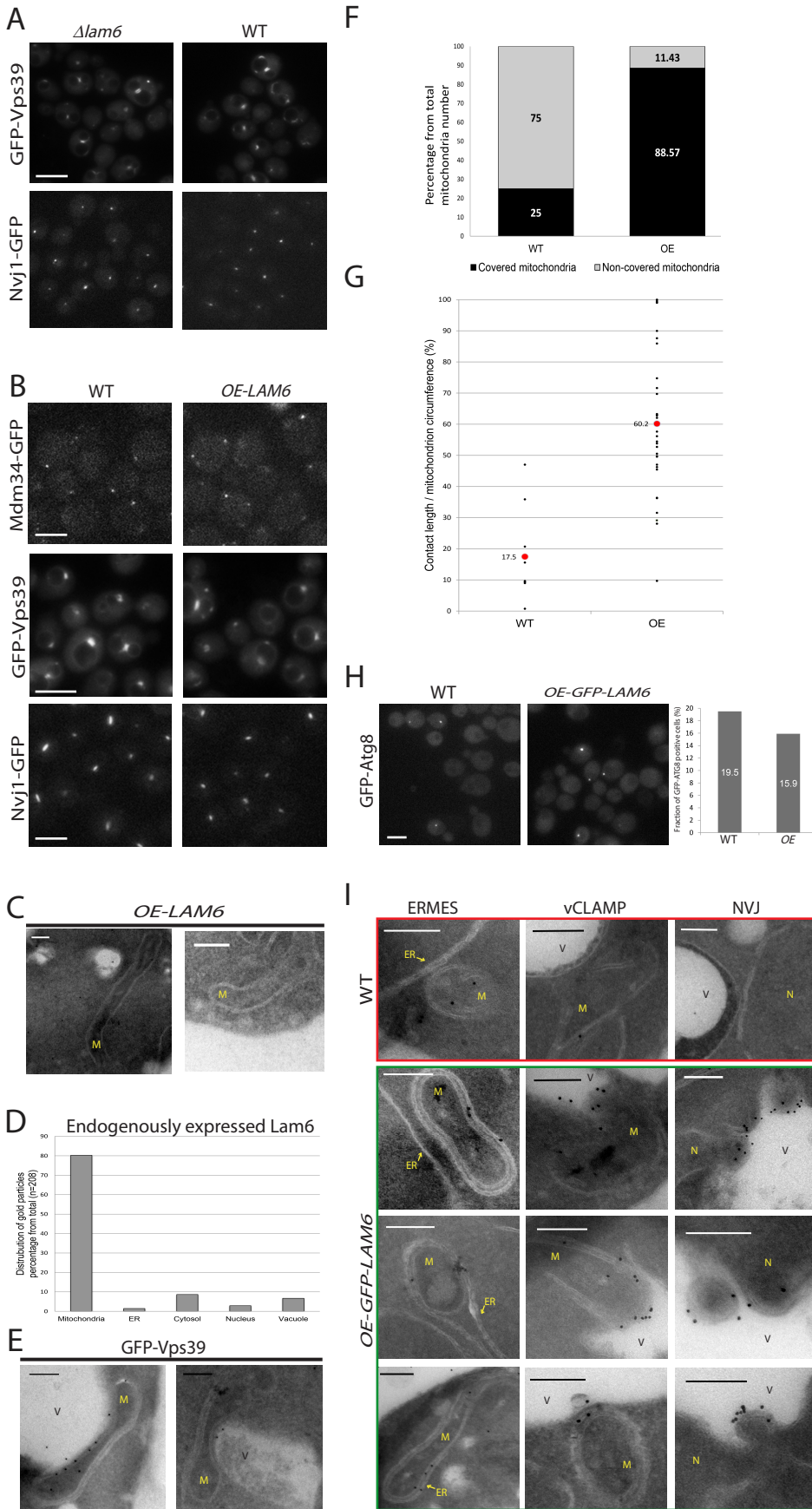


Figure S3: Overexpression of tagged Lam6 increases the extent of contact sites. Related to figure 3.

(A) Deletion of *LAM6* did not prevent the formation of NVJ (marked by Nvj1-GFP) or vCLAMP (marked by GFP-Vps39), confirming that Lam6 is not required for the formation of these contact sites. Bar = 5 μm . (B) Overexpression of the non-tagged form of Lam6 did not affect the extent of the three contact sites: ERMES (marked by Mdm34-GFP), vCLAMP (marked by Vps39) and NVJ (marked by Nvj1-GFP). Bar = 5 μm . (C) Replacing the endogenous promoter of Lam6 with a constitutive one alone did not result in the same expansion of the ER-mitochondria contact sites as in the case of overexpression of GFP-Lam6. Mitochondria were not surrounded with ER tubules in this condition. Bar = 200 nm. (D) Graph showing distribution analysis of gold particles in immunoelectron microscopy analysis of an Lam6-GFP strain, using an antibody against GFP. Lam6 accumulates specifically in mitochondria most probably representing ERMES contacts. (E) Upon overexpression of GFP-Lam6 instances in which vacuoles and mitochondria were found in close proximity were markedly higher. The vCLAMPs were validated by Immuno-labeling GFP-Vps39. Bar = 200 nm. (F) The number of mitochondrion that had visible contact with ER, in the endogenously expressed Lam6 strain and in the overexpressing GFP-Lam6 strain, was calculated. Bars represent the percentage of mitochondria that had contact with ER from the total mitochondria number (for WT n=36, for OE n=35). (G) The length of the contact site was measured and the percentage of the contact length out of the total circumference of the mitochondria was calculated. The average percentage is shown in red for the endogenously expressing and overexpressing GFP-Lam6 strains. (H) Fluorescence microscopy imaging of the

autophagy regulator Atg8. GFP-Atg8 levels did not increase upon overexpression of GFP-Lam6, confirming that the membranes surrounding the mitochondria are not part of autophagosomes. Bar = 5 μ m. (I) Additional images from immunoelectron microscopy of Lam6 overexpression (supplementing Figure 3B). N, nucleus, M, mitochondria, V, Vacuole. Bar = 200 nm.

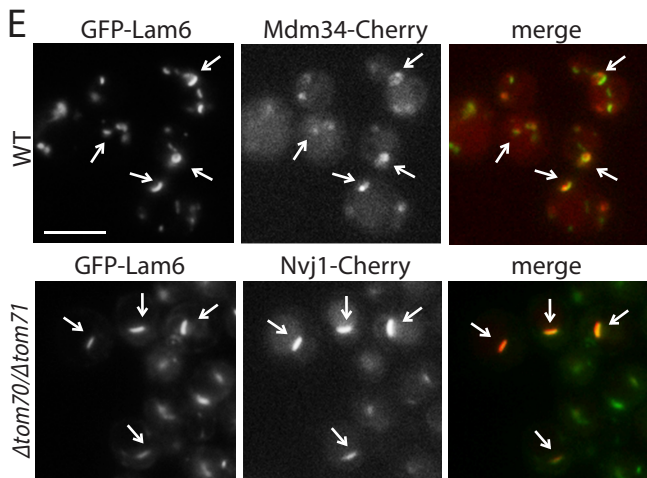
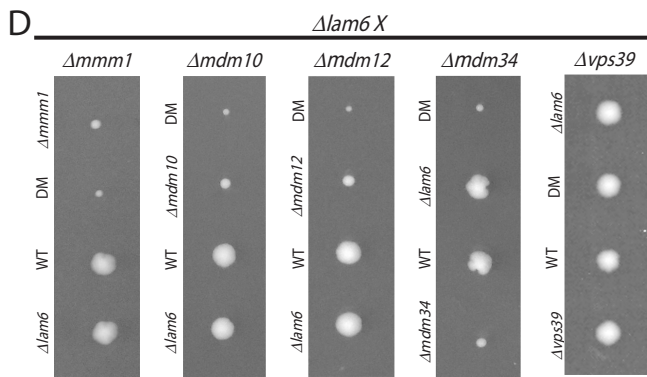
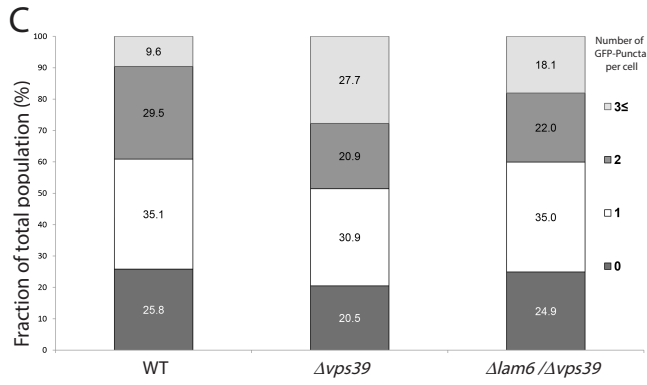
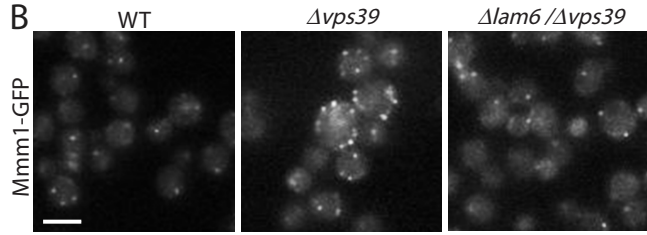
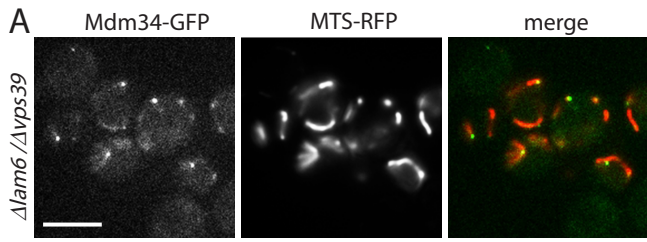


Figure S4: Lam6 is important for cross-talk between contact sites. Related to figure 4 and to the discussion.

(A) When deleting both *LAM6* and *VPS39*, the ERMES subunit Mdm34-GFP remained co-localized with mitochondria. Bar = 5 μ m. (B) Fluorescent microscopy demonstrating that the ERMES contact (as measured by the number of Mmm1-GFP puncta per cell, supplementing Figure 4A where the same experiment was performed with Mdm34-GFP) expanded in the $\Delta vps39$ background relative to WT. However the expansion did not occur on the background of $\Delta vps39 \Delta lam6$ demonstrating that Lam6 is necessary for ERMES expansion under these conditions. Bar = 5 μ m. (C) Quantitation of (B). Bars represent the percentage of cells containing specific number of puncta/cell out of total cells counted for the strain (for WT n=271 cells, for $\Delta vps39$ n=278, for $\Delta vps39 \Delta lam6$ n=277). (D) $\Delta lam6$ strain was crossed with strains containing a deletion in each of the ERMES subunits or $\Delta vps39$ to create diploids. Tetrad analysis of ascospores resulting from meiosis of those diploids demonstrate that in all cases combination of mutations in both *LAM6* and ERMES subunits resulted in decreased growth (synthetic sick phenotype) when comparing them to either single mutants. In contrast, mutants for Lam6 and Vps39 were not synthetic sick. (E) In WT cells most of the overexpressed GFP-Lam6 co-localized with ERMES (Mdm34). Deletion of Tom70 and Tom71 resulted in complete relocalization of Lam6 to the NVJ, as marked by Nvj1-Cherry. Bar = 5 μ m.

Supplemental Figure legends:

Table S1: Protein-protein interaction analysis of Mdm10, Mdm12, Mdm34 and Mmm1. Related to figure 1.

Expression levels are given as label-free quantification (LFQ) normalized intensities. Significant binders (marked with +) were extracted with a Welch's test with permutation based FDR=0.05 and S0=0.5. For each test the p-values (-log value) and the test difference are provided.

Table S2: Protein-protein interaction analysis of Lam6. Related to figure 1.

Expression levels are given as label-free quantification (LFQ) normalized intensities. Significant binders (marked with +) were extracted with a Welch's test with permutation based FDR=0.05 and S0=0.5. For each test the p-values (-log value) and the test difference are provided.

Table S3: Yeast strains used in this study. Related to figures 1-4.

Yeast strains created and used in this study are listed in the table. All yeast strains in this study are based on the BY4741 laboratory strains (Brachmann et al., 1998).

Supplemental Experimental Procedures

Electron microscopy

For immunoelectron microscopy cells were fixed in 4% paraformaldehyde with 0.1% glutaraldehyde in 0.1M cacodylate buffer (pH=7.4), for 1 hour at room temperature and kept at 4°C during 1-2 days. The samples were soaked overnight in 2.3 M sucrose and rapidly frozen in liquid nitrogen. Frozen ultrathin (70-90 nm) sections were cut with a diamond knife at -120°C on an EM UC6 ultramicrotome (Leica Microsystems, Vienna, Austria). The sections were collected on 200-mesh formvar coated nickel grids. Sections were blocked by a blocking solution containing 0.5% BSA, 0.2% glycine, 0.5% gelatin and 0.1% Tween-20. Immuno-labeling was performed using rabbit polyclonal anti-GFP antibody (ab6556, 1:100; Abcam) during 1.5-2 hours at room temperature (RT) followed by goat anti-rabbit IgG coupled to 10-nm gold particles (1:20 dilution) 30 min at RT. Contrasting and embedding were performed as described (Tokuyasu, 1986). The embedded sections were scanned and digitally viewed on transmission electron microscopes Tecnai Spirit (FEI, Eindhoven, the Netherlands) at 120kV using a CCD Eagle camera with TIA software (FEI) or Tecnai T12 electron microscope (FEI) operating at 120 kV. Images were recorded with an ErlangshenES500W CCD camera (GATAN).

Of note, although gold particles appeared inside the mitochondria, the labeling most probably represent ERMES contact sites, reminiscent of the fluorescence microscopy pattern, and the appeared mislocalization is the result of the slicing plane as well as antibody size.

In electron micrographs, vacuoles may appear as black areas of condensed vacuolar content or as white areas where the vacuoles were before they collapsed and detached from the slide (Guthrie and Fink, 2002).

Isolation of microsomal fractions

Pull downs of individual ERMES components (Mmm1-3HA, Mdm34-3HA, Mdm12-3HA and Mdm10-3HA) for LC-MS/MS were performed from microsomal fractions. Sucrose-density-gradient purification of microsomes was performed essentially as described by (Wuestehube and Schekman, 1992). Strains were grown in YPD media to $OD_{600} \sim 1$, then harvested and washed once in 100 mM Tris-HCl pH 9.4, 10 mM dithiothreitol (DTT). Cells were then re-suspended in 0.7M sorbitol, 10mM Tris-HCl pH 7.4 buffer supplemented with 1.5% (w/v) bactopectone, 0.75% (w/v) yeast extract and 0.5% (w/v) glucose. Spheroplasts were generated by adding 3mg Zymolase (MP Biomedicals) and isolated by centrifugation through a 0.8 M sucrose cushion. Spheroplast pellet was re-suspended in lysis buffer (0.1M sorbitol, 20 mM HEPES, pH 7.4, 50 mM potassium acetate, 2 mM ethylenediaminetetraacetic acid (EDTA), 1 mM DTT and protease inhibitors (Sigma) and subjected to 25 strokes in a Dounce homogenizer. The resulting homogenate was centrifuged at 1000g and the combined low-speed supernatant was centrifuged at 27,000 g (Ti60 rotor; Beckman Instruments). The membrane fraction was then collected, re-suspended in lysis buffer and fractionated through a 2-step sucrose gradient of 1.2 M and 1.5 M sucrose by centrifugation at 100,000 g (SW41 rotor; Beckman Instruments) for 1 hour at 4°C. The microsomal fraction residing at the gradient interface was collected, washed and re-suspended in reaction buffer (20 mM HEPES pH 6.8, 150 mM potassium acetate, 5 mM magnesium acetate, 250 mM Sorbitol). Total protein concentration of every sample was determined using BCA reagent (Thermo Scientific).

Isolation of mitochondria-enriched fractions

Pull down of Lam6-GFP and GFP-Lam6 for LC-MS/MS analysis was performed from mitochondria-enriched preparations. Isolation of mitochondria-enriched fractions was performed

essentially as previously published (Daum et al., 1982). Briefly, strains were grown in YPD media to $OD_{600} \sim 1$, then harvested and washed once in 100 mM Tris-HCl pH 9.4, 10 mM DTT. Cells were then re-suspended in sorbitol buffer (1.2M sorbitol, 20mM KPi buffer pH 7.4). Spheroplasts were generated by adding 3 mg Zymolase, until 95% of cells were converted into spheroplasts according to OD measurement (normally takes 40-45 min) (MP Biomedicals), washed in same buffer and isolated by centrifugation 5 min at 2000g at 4°C. Spheroplast pellet was re-suspended in homogenization buffer (0.6 M sorbitol, 20 mM HEPES, pH 7.4 and protease inhibitors (Sigma)) and subjected to 15 strokes in a Dounce homogenizer. The resulting homogenate was centrifuged at 800 g and the combined low-speed supernatant was centrifuged at 12,000 g for 15 min at 4°C (SS-34 rotor; Sorvall). The membrane fraction was then collected, re-suspended in sucrose buffer (250 mM sucrose, 10 mM HEPES pH 7.4 supplemented with protease inhibitors) and aliquoted. Total protein concentration of every sample was determined using BCA reagent (Thermo Scientific).

Interaction proteomics

Pull down of individual ERMES components from microsomal fractions (Mmm1-3HA, Mdm34-3HA, Mdm12-3HA and Mdm10-3HA), or LAM6-GFP from mitochondria-enriched preparations was performed as follows: fractions with 5 mg total protein were solubilized in 15mM Tris-HCl pH 7, 150 mM NaCl, 3% digitonin and protease inhibitors (Sigma P8215) for 1 hour on ice.

Samples containing HA-tagged ERMES components were incubated with μ MACS anti-HA beads (Miltenyi Biotec, Germany), while LAM6-GFP was incubated with GFP-trap agarose beads (Chromotek, Germany) for 45' followed by three washes with 150 mM NaCl, 15 mM Tris HCl pH 7. Elution was performed through on-bead digestion, by 2h incubation of the beads with 100 μ l of 2 M urea, 50 mM Tris HCl pH 7.5, 1 mM DTT and 0.4 μ g sequencing grade trypsin,

followed by an additional wash with 2 M urea, 50 mM Tris HCl pH 7.5 and 5 mM iodoacetamide. Eluates were combined and incubated over night at room temperature. Resulting peptides were acidified with Trifluoroacetic acid (TFA) and purified on C18 StageTips (Rappsilber et al., 2007). LC-MS/MS analysis was performed on the EASY-nLC1000 UHPLC (Thermo Scientific) coupled to the Q-Exactive mass spectrometer (Thermo Scientific). Peptides were loaded onto the column with buffer A (0.5% acetic acid) and separated on a 50 cm PepMap column (75 μ m i.d. 2 μ m beads; Dionex) using a 4 h gradient of 5-30% buffer B (80% acetonitrile, 0.5% acetic acid). Raw MS files were analyzed with MaxQuant (Cox and Mann, 2008) using the label-free algorithm for protein quantification (Cox et al., 2014). Significant interactors were extracted based on the statistical difference between the label-free quantification (LFQ) intensities of the proteins in the pull down of specific proteins and the control strains without HA-tag expression. One-sided Welch's test was performed with 0.05 permutation-based false discovery rate (FDR) and $S_0=0.5$ (Tusher et al., 2001).

Isolation of mitochondrial enriched fractions followed by western blot

Yeast strains BY4741 (WT) and $\Delta lam6::Kan$, were grown at 30 °C in YPD medium (1% yeast extract; 2% bactopectone, 2% glucose, pH 5.0 (HCl)) to mid-logarithmic phase. Mitochondria were isolated by differential centrifugation (Meisinger et al., 2006). Mitochondrial proteins (10 - 50 μ g) were separated by Tricine-SDS-PAGE (Schägger, 2006) and transferred onto polyvinylidene difluoride (PVDF) membranes. Proteins were detected by immunodecoration with rabbit antibodies against the indicated proteins followed by incubation with goat anti-rabbit IgG peroxidase conjugate (A6154, 1:5000, Sigma, St. Louis, MO, USA) and visualized by enhanced chemiluminescence (Haan and Behrmann, 2007) using the LAS imaging system (Fujifilm).

Flow cytometry

Yeast cells grown to mid-log in liquid synthetic media (SD) and flow cytometry analysis was performed using a BD LSR II flow cytometer (BD Biosciences). Results were analyzed using BD FACSDiva software.

Supplemental References

- Brachmann, C.B., Davies, A., Cost, G.J., Caputo, E., Li, J., Hieter, P., and Boeke, J.D. (1998). Designer deletion strains derived from *Saccharomyces cerevisiae* S288C: a useful set of strains and plasmids for PCR-mediated gene disruption and other applications. *Yeast* *14*, 115–132.
- Cox, J., and Mann, M. (2008). MaxQuant enables high peptide identification rates, individualized p.p.b.-range mass accuracies and proteome-wide protein quantification. *Nat. Biotechnol.* *26*, 1367–1372.
- Cox, J., Hein, M.Y., Lubner, C.A., Paron, I., Nagaraj, N., and Mann, M. (2014). MaxLFQ allows accurate proteome-wide label-free quantification by delayed normalization and maximal peptide ratio extraction. *Mol. Cell. Proteomics* *13*, 2513–2526.
- Daum, G., Böhni, P.C., and Schatz, G. (1982). Import of proteins into mitochondria. Cytochrome b2 and cytochrome c peroxidase are located in the intermembrane space of yeast mitochondria. *J. Biol. Chem.* *257*, 13028–13033.
- Guthrie, C., and Fink, G.R. (2002). *Guide to Yeast Genetics and Molecular and Cell Biology: Part C* (Gulf Professional Publishing).
- Haan, C., and Behrmann, I. (2007). A cost effective non-commercial ECL-solution for Western blot detections yielding strong signals and low background. *J. Immunol. Methods* *318*, 11–19.
- Meisinger, C., Pfanner, N., and Truscott, K.N. (2006). Isolation of yeast mitochondria. *Methods Mol. Biol.* *313*, 33–39.
- Rappsilber, J., Mann, M., and Ishihama, Y. (2007). Protocol for micro-purification, enrichment, pre-fractionation and storage of peptides for proteomics using StageTips. *Nat. Protoc.* *2*, 1896–1906.
- Schägger, H. (2006). Tricine-SDS-PAGE. *Nat. Protoc.* *1*, 16–22.
- Tokuyasu, K.T. (1986). Application of cryoultramicrotomy to immunocytochemistry. *J. Microsc.* *143*, 139–149.
- Tusher, V.G., Tibshirani, R., and Chu, G. (2001). Significance analysis of microarrays applied to the ionizing radiation response. *Proc. Natl. Acad. Sci. U. S. A.* *98*, 5116–5121.
- Wuestehube, L.J., and Schekman, R.W. (1992). Reconstitution of transport from endoplasmic reticulum to Golgi complex using endoplasmic reticulum-enriched membrane fraction from yeast. *Methods Enzymol.* *219*, 124–136.